Hindawi Publishing Corporation
Journal of Nanomaterials
Volume 2011, Article ID 654715, 6 pages
doi:10.1155/2011/654715

Research Article

Mesoporous In_2O_3: Effect of Material Structure on the Gas Sensing

Z. X. Cheng,[1] X. H. Ren,[1] J. Q. Xu,[1,2] and Q. Y. Pan[1]

[1] *Department of Chemistry, College of Science, Shanghai University, Shanghai 200444, China*
[2] *State Key Laboratory of Transducer Technology, Shanghai Institute of Microsystem and Information Technology, Chinese Academy of Sciences, Shanghai 200050, China*

Correspondence should be addressed to Z. X. Cheng, zxcheng@staff.shu.edu.cn

Received 14 September 2010; Revised 10 February 2011; Accepted 26 February 2011

Academic Editor: Claude Estournes

We present a semiconductor gas sensor based on mesoporous In_2O_3 (m-In_2O_3). The m-In_2O_3 was successfully fabricated by a simple sol-gel process, using block copolymer PE6800 as a soft template. The results of gas sensing reveal that the m-In_2O_3 prepared at room temperature shows higher resistance, which plays the key role in its greater sensitivity. The pore structure of material has an influence on gas adsorption on the material surface, which further affects response-recovery time of gas sensor.

1. Introduction

Over the past few years, mesoporous materials have received considerable attention due to their many attractive characteristics, such as well-ordered pore systems, large specific surface areas, high thermal stability, and these noble characteristics lead to their various areas of application including molecular separation [1], heterogeneous catalysis [2], nanocomposite preparation [3, 4], and gas sensors [5, 6].

In recent years, many mesoporous oxide materials like Al_2O_3, WO_3, ZrO_2 have been successfully synthesized [7, 8]. However, the research on m-In_2O_3 is still quite sparse. To our best knowledge, In_2O_3 is an n-type semiconductor with a wide bandgap close to GaN (3.5–3.7 eV) that shows the unusual combination of good optical transparency in the visible region and high electrical conductivity. Besides, In_2O_3 is also a promising gas sensing material for various oxidizing gases, such as O_3 [9, 10], O_2 [11], or nitric oxides [12, 13], as well as for reducing gases like CO or H_2 [14, 15].

As we all know, the working principle of gas-sensing materials is based on measurement of gas adsorption and the changes of the conductivity caused by the surface reaction process. Increased surface area can improve the response performance. Therefore, the application of mesoporous materials can enhance the gas sensing performance owing to their large specific surface area. Though some examples of m-In_2O_3 have already been reported [16–18], little attention has been paid to study the effect of material structure on the gas-sensing performance. Herein, we successfully synthesized m-In_2O_3 with different structures by controlling the temperature during preparing process and investigated the effect of pore structure on the gas sensing performance.

2. Experimental Section

All the analytical chemicals were purchased from Shanghai Chemical Industrial Co. Ltd. (Shanghai, China), except for amphiphilic triblock copolymer PE6800, poly(ethylene oxide)-poly(propylene oxide)-poly (ethylene oxide) (EO_{73}-PO_{28}-EO_{73}, Mw=8050), obtained from BASF and used without further purification.

2.1. Synthesis. The m-In_2O_3 materials, utilized amphiphilic triblock copolymer PE6800 as a soft template to control their morphology, were synthesized according to a literature produced [18].

In a typical synthesis, 0.01 mol of $InCl_3 \cdot 4H_2O$ was introduced into the 100 mL aqueous solution which contains 1 wt% triblock copolymer PE6800. Afterwards, the ammonia was dropped into the solution at 25°C, and the pH value of the final solution was controlled at 6.5. The mixed solution was then gently shaken until intimate mixing, and then

Table 1: Analysis of m-In_2O_3 obtained at different temperatures in the field of BET test.

Sample	Reaction temperature (°C)	Morphology	Particles size (nm)	Specific surface area ($m^2 \cdot g^{-1}$)	Pore volume ($cm^3 \cdot g^{-1}$)	Pore diameter (nm)	
M-1	25	Mesoporous particles	~30	54.78	0.346	3	32
M-2	40	Mesoporous particles	~50	62.82	0.403	6	50

white latex-like solution was obtained. After that, the above solution was aged for 3 days; subsequently the precipitate was poured out after centrifugal separating and washed with deionized water until no chloride ions were detected. Next, the products were dried overnight. Ultimately, the dried sample was calcined at 500°C for 2 hours to remove the surfactant (namely product-M-1), and the other product was prepared in the identical process at 40°C (namely, product-M-2).

2.2. Gas-Sensing Properties Research. The gas sensor was prepared, and the gas response was measured in the static state. Paste of In_2O_3 powders was coated onto an alumina ceramic tube attached with a pair of Au electrodes. The sensors were calcined at 500°C for 2 h to provide good mechanical strength and to remove the organic additives. Finally, a small Ni-Cr alloy heating coil was inserted into the tube to form a heater. The sensor should be kept at its working temperature for aging several days to evaluate the long-term stability. The electrical resistance of a sensor was measured in air and in detected gases. The gas-sensing responses of the material to C_2H_5OH, CH_3OH, NH_3, and NO_2 gases were studied and correlated with the structural properties of the active materials.

3. Results and Discussion

3.1. Characterization of m-In_2O_3 Powders. XRD analysis is the most useful technique for identification of crystalline structure of the sample. Figure 1 displays wide-angle XRD of m-In_2O_3 synthesized at different temperatures after calcinations at 500°C for 2 h. The intensities and locations of the peaks were identified as a cubic structure of In_2O_3 (JCPDS card 6-0416). No impure peaks were observed in the wide-angle XRD patterns, which indicated high purity of the sample. From the patterns, it is perceptible that as the reaction temperature increased, the intensities of peak (222) to (400), (222) to (440) were enhanced, accordingly, which were larger than those of standard ratio. The surfactant PE6800 was found to be as a structure directing agent. Furthermore, the role of structure-oriented was boost up as the reaction temperature increased, which was in agreement with the results suggested by Yu et al. [19] using P123-synthesized mesoporous molecular sieves.

Low-angle XRD patterns, shown in Figure 2, exhibit a single XRD peak at $2\theta = 0.61°$ and 0.62°, respectively, which confirm that the materials synthesized at different

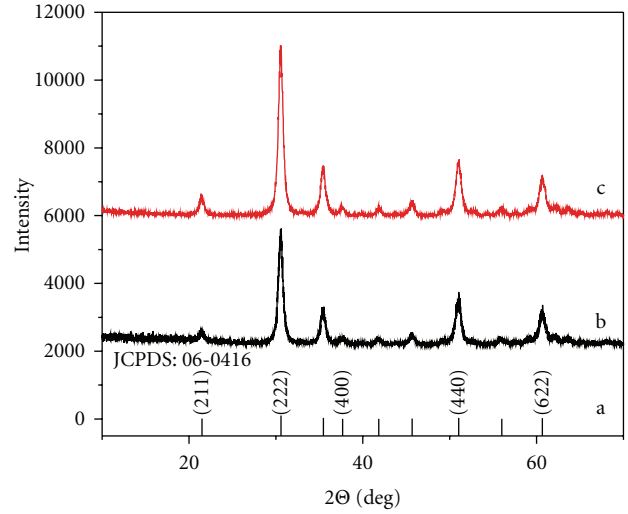

Figure 1: Wide-angle XRD pattern of the m-In2O3 prepared at different temperatures: (a) standard atlas, (b) 25°C, (c) 40°C.

temperatures both have been occupied by the mesopore cavums. However, the single XRD peak indicates slightly lower overall nanostructural order or smaller coherent scattering domains. This is also confirmed by N_2 adsorption and desorption isotherm (Figure 1), and the structural parameters are included in Table 1.

A more detailed analysis of the fine structure of the m-In_2O_3 (not allowed by the XRD) was obtained by High-Resolution Transmission Electron Microscopy (HRTEM), Field Emission Scanning Electron Microscopy (FE-SEM).

HRTEM images as depicted in Figure 3 clearly indicate that samples scattered evenly with an average diameter of 30 nm and 50 nm synthesized at 25°C and 40°C, respectively, which is well consistent with the results of XRD analysis.

FE-SEM image (Figure 4(a)) clearly shows that extremely aggregated nano particles with 30 nm were produced. Moreover, it can be seen that the product has mesoporous structures. The diameter of nano particles is up to 50 nm, and the structures of the mesoporous In_2O_3 are preserved without appreciable change when the reaction temperature was increased to 40°C, as shown in Figure 4(b).

As can be seen from Table 1, the structure of m-In_2O_3 is affected slightly by the reaction temperature. Both products are in round particle size; however, the related parameter increased as the temperature rises which was shown in Table 1.

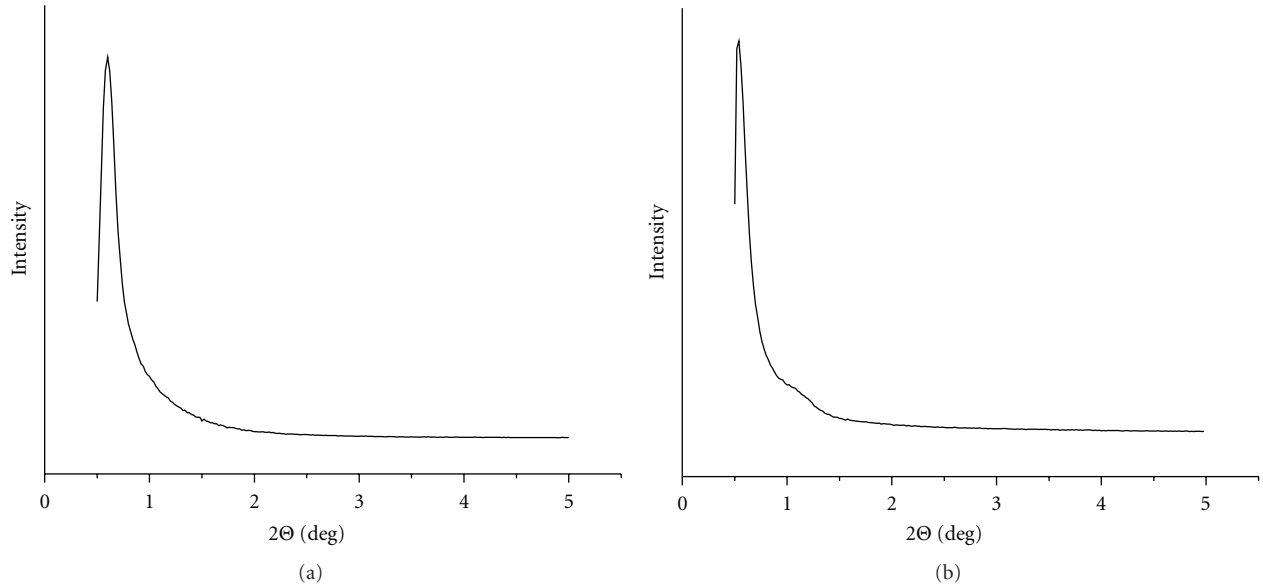

Figure 2: Low-angle XRD patterns of the m-In_2O_3 prepared at different temperatures: (a) 25°C, (b) 40°C.

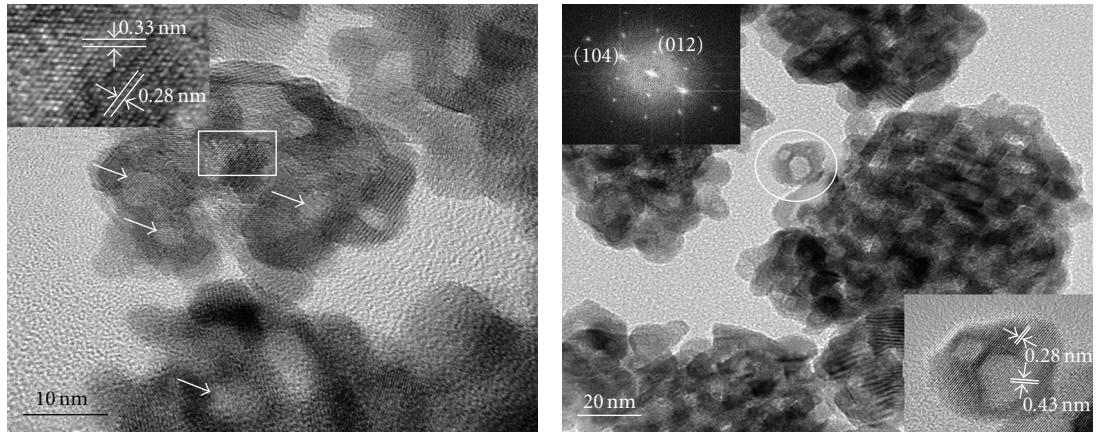

(a) (b)

Figure 3: HRTEM image of the mesoporous In_2O_3 synthesized at different temperatures: (a) 25°C, (b) 40°C.

Table 1 shows that the specific surface area of M-1 (54.78 m^2g^{-1}) is smaller than that of M-2 (62.82 m^2g^{-1}). The average diameter of the crystals can be estimated as about 30 nm, 50 nm, respectively. Generally, mesoporous material with the smaller pore size enables larger specific surface area. However, we find an opposite result that M-1 has smaller pore diameter than M-2, and specific surface area of M-1 is still smaller. So, we thought the result was concerned with the structure of bimodal pore size distribution. In Figure 5, we see that the rate of small pores is lower in M-1 than in M-2, which is beneficial for enlarging specific surface area.

Then N_2 adsorption and desorption isotherm for m-In_2O_3 of different reaction temperatures can be seen in Figure 5. The BJH pore size distribution curve showed that the pore size of M-1 was mainly in the range of 2–8 nm and 12–48 nm, whilethat of M-2 was mainly in the range of 4–10 nm and 20–60 nm, which matched well with the results of N_2 adsorption and desorption isotherm. Simultaneously, the BET surface areas are 54.78 m^2/g and 62.82 m^2g^{-1}, respectively.

The N_2 adsorption-desorption isotherm of samples made by different reaction temperatures for m-In_2O_3 is markedly dissimilar, which indicated that the pore structures of these two samples are different. In this case, the process of gas adsorption on the material surface is varied, and it further affects response-recovery time of gas sensor.

3.2. Sensing Properties of Gas Sensor. We have fabricated chemical sensors successfully with as-prepared nano architectures. Firstly, the gas response was measured in the static state under different operating temperatures. The results were shown in Figure 6, and m-In_2O_3 showed excellent

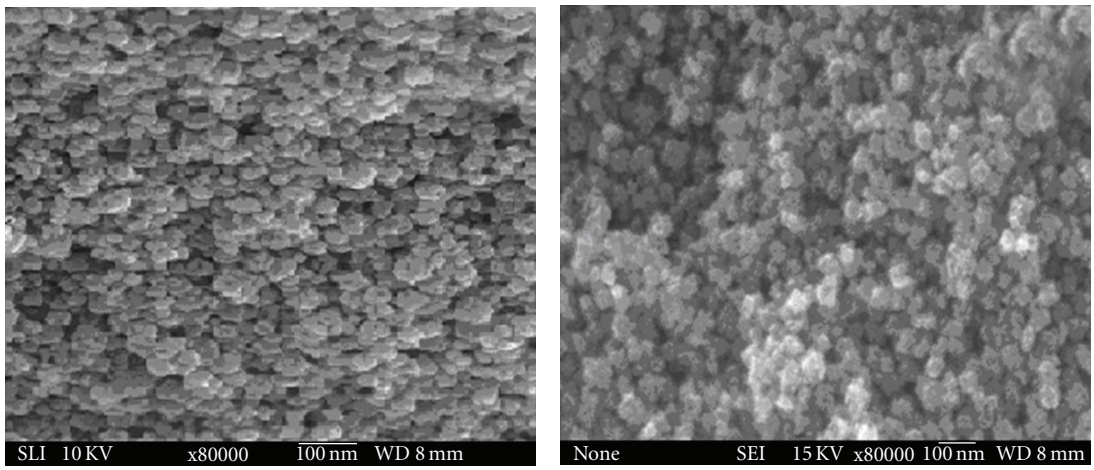

(a) (b)

Figure 4: FE-SEM image of the mesoporous In_2O_3 synthesized at different temperatures: (a) 25°C, (b) 40°C.

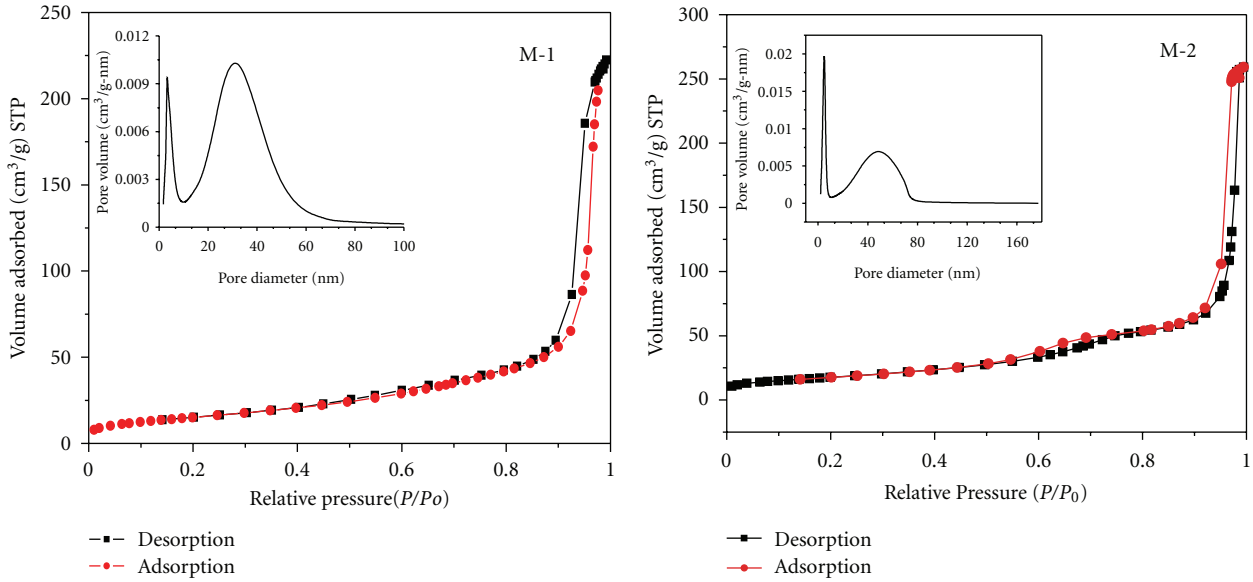

(a) (b)

Figure 5: N_2 adsorption-desorption isotherm at 77 K for m-In_2O_3 prepared at different temperatures. The pore size distributions.

gas-sensing properties to these tested gases. As shown in Figure 6, the sensitivities of m-In_2O_3 to C_2H_5OH, CH_3OH, and NO_2 are higher than those of HCHO in the testing gases. In addition, M-1 synthesized at 25°C performed higher sensitivity compared to 40°C (except NO_2).

Accordingly, we can obtain that the resistance of materials in the air plays a key role in their response. In this paper, the response (S) of the sensor is defined as $S = R_a/R_g$ (for reducing gas), where R_a and R_g are the resistances of the sensors in the testing gas/air mixture and in air, respectively, so the bigger resistance in air will induce the higher sensitivity. Generally, the response of surface adsorption-controlled materials depends on specific surface area of materials, that is, the larger the specific surface area is, the higher sensitivity it achieves, which is contrary to the experimental results. In order to explain the abnormal phenomenon, the components of resistance in the air were studied, which was shown in Figure 7.

In Figure 7 the resistance of the two materials presented consistent change as the heating temperature increased, which shows typical characteristic of surface adsorption-controlled materials. However, M-1 is of higher resistance clearly than that of M-2. It could be assessed that M-1 prepared at lower temperature has higher surface activity, because surface-bound oxygen atoms are able to abstract the electron easier from the material, thus the surface

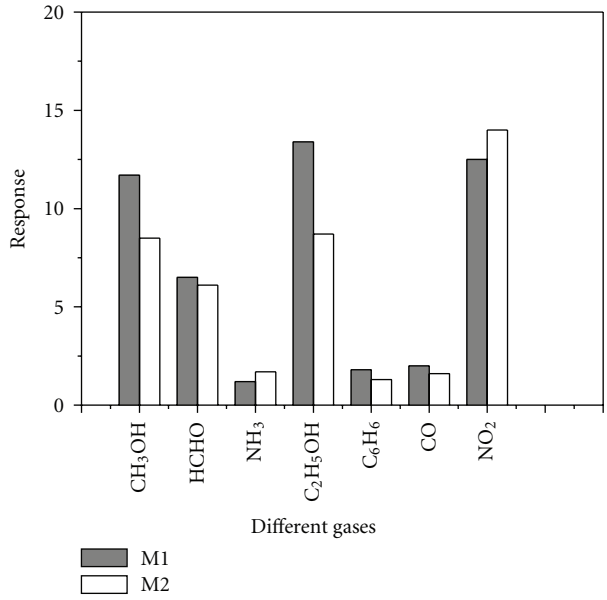

Figure 6: Effect of reaction temperature on gas response of m-In_2O_3-based gas sensor at optimal working temperature.

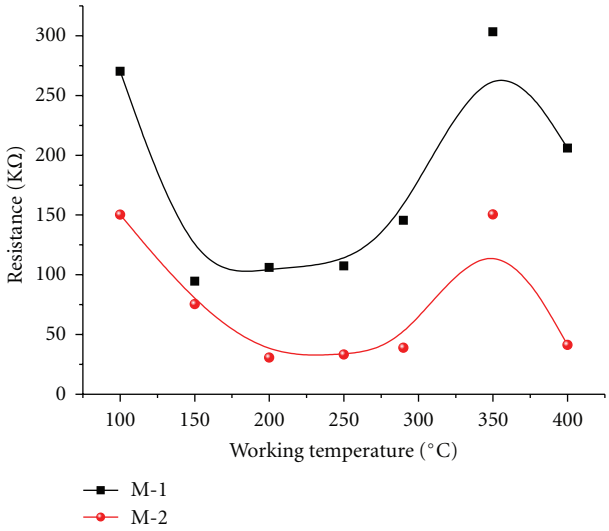

Figure 7: The resistance-temperature curves of m-In_2O_3 prepared at different temperatures.

electron potential barrier increased, causing the resistance of materials in air to be increased, thereby the sensitivity of the material enhanced.

The response and recovery time of our sensors has also been investigated. Here the response time is defined as the time required for the sample variation resistance to reach 90% of the equilibrium value following a step increase in the test gas concentration, while the recovery time is defined as the time necessary for the sample to return to 10% above its original resistance in air following the zeroing of the test gas. Figure 8 shows the response-recovery curve of m-In_2O_3 prepared to 50 ppm of C_2H_5OH. It can be seen that the response times are both in 5 s, whereas recovery times are

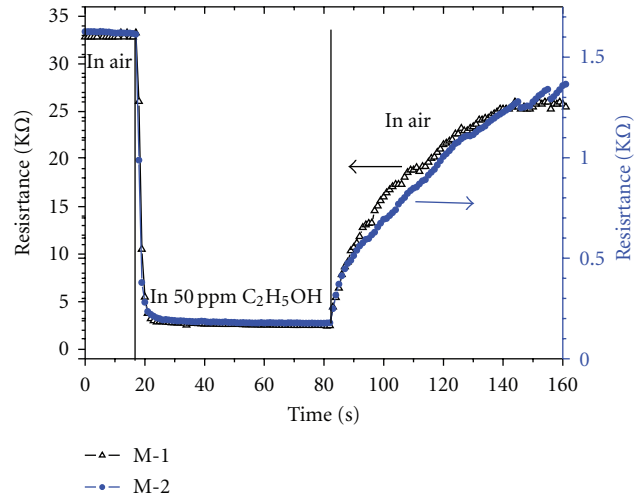

Figure 8: The response-recovery curve of m-In_2O_3 prepared at different temperatures on the response to C_2H_5OH.

totally different. M-1 showed faster recovery time than M-2. Combined with BET tests (see Figure 5), we find that the M-1 mainly cause the occurrence of single-molecule adsorption and with easy desorption of target gases, which leads to very short recovery time. M-2 with multi-molecular layers adsorption shows a larger recovery value. In summary, the m-In_2O_3synthesized at room temperature has better gas-sensing properties.

4. Conclusions

In summary, the pore structure of nanomaterial plays a vital role in the application of semiconducting metal oxides as gas sensors. The m-In_2O_3 prepared at room temperature performs greater sensitivity, which plays the key role in its better gas-sensing properties. The pore structure of material has an influence on gas adsorption on the material surface and further affects response-recovery time of gas sensor.

Acknowledgments

This work was supported by the National Nature Science Foundation of China (no. 61071040, 50872142), the Leading Academic Discipline Project of Shanghai Municipal Education Commission (no. J50102), and Innovation Fund of Shanghai University (2010). The authors also thank the Analysis and Research Center at Shanghai University for sample characterization.

References

[1] J. M. Kisler, A. Dähler, G. W. Stevens, and A. J. O'Connor, "Separation of biological molecules using mesoporous molecular sieves," *Microporous and Mesoporous Materials*, vol. 44-45, pp. 769–774, 2001.

[2] X. He and D. Antonelli, "Recent advances in synthesis and applications of transition metal containing mesoporous molecular sieves," *Angewandte Chemie - International Edition*, vol. 41, no. 2, pp. 214–229, 2002.

[3] W. S. Chae, Y. R. Kim, and J. S. Jung, "Structural confinement effects of ternary chalcogenide in mesoporous ALMCM-41 of different pore diameters," *Journal of Physical Chemistry B*, vol. 107, no. 7, pp. 1585–1591, 2003.

[4] H. Parala, H. Winkler, M. Kolbe et al., "Confinement of CdSe nanoparticles inside MCM-41," *Advanced Materials*, vol. 12, no. 14, pp. 1050–1055, 2000.

[5] T. Wagner, T. Waitz, J. Roggenbuck, M. Fröba, C. D. Kohl, and M. Tiemann, "Ordered mesoporous ZnO for gas sensing," *Thin Solid Films*, vol. 515, no. 23, pp. 8360–8363, 2007.

[6] Y. Shimizu, A. Jono, T. Hyodo, and M. Egashira, "Preparation of large mesoporous SnO_2 powder for gas sensor application," *Sensors and Actuators, B*, vol. 108, no. 1-2, pp. 56–61, 2005.

[7] P. Yang, D. Zhao, D. I. Margolese, B. F. Chmelka, and G. D. Stucky, "Block copolymer templating syntheses of mesoporous metal oxides with large ordering lengths and semicrystalline framework," *Chemistry of Materials*, vol. 11, no. 10, pp. 2813–2826, 1999.

[8] P. Yang, D. Zhao, D. I. Margolese, B. F. Chmelka, and G. D. Stucky, "Generalized syntheses of large-pore mesoporous metal oxides with semicrystalline frameworks," *Nature*, vol. 396, no. 6707, pp. 152–155, 1998.

[9] A. Gurlo, N. Barsan, U. Weimar, M. Ivanovskaya, A. Taurino, and P. Siciliano, "Polycrystalline well-shaped blocks of indium oxide obtained by sol-gel method and their gas-sensing properties," *Chemistry of Materials*, vol. 15, no. 23, pp. 4377–4383, 2003.

[10] M. Z. Atashbar, B. Gong, H. T. Sun, W. Wlodarski, and R. Lamb, "Investigation on ozone-sensitive InO thin films," *Thin Solid Films*, vol. 354, no. 1, pp. 222–226, 1999.

[11] G. Neri, A. Bonavita, G. Micali, G. Rizzo, N. Pinna, and M. Niederberger, "InO and Pt-InO nanopowders for low temperature oxygen sensors," *Sensors and Actuators, B*, vol. 127, no. 2, pp. 455–462, 2007.

[12] S. Bianchi, E. Comini, M. Ferroni, G. Faglia, A. Vomiero, and G. Sberveglieri, "Indium oxide quasi-monodimensional low temperature gas sensor," *Sensors and Actuators, B*, vol. 118, no. 1-2, pp. 204–207, 2006.

[13] M. Ivanovskaya, A. Gurlo, and P. Bogdanov, "Mechanism of O and NO detection and selectivity of InO sensors," *Sensors and Actuators, B*, vol. 77, no. 1-2, pp. 264–267, 2001.

[14] J. T. McCue and J. Y. Ying, "SnO_2-In_2O_3 nanocomposites as semiconductor gas sensors for CO and NOx Detection," *Chemistry of Materials*, vol. 19, no. 5, pp. 1009–1015, 2007.

[15] Z. Zhan, D. Jiang, and J. Xu, "Investigation of a new In_2O_3-based selective H_2 gas sensor with low power consumption," *Materials Chemistry and Physics*, vol. 90, no. 2-3, pp. 250–254, 2005.

[16] T. Waitz, T. Wagner, T. Sauerwald, C. D. Kohl, and M. Tiemann, "Ordered mesoporous InO: synthesis by structure replication and application as a methane gas sensor," *Advanced Functional Materials*, vol. 19, no. 4, pp. 653–661, 2009.

[17] J. Huang and L. Gao, "Synthesis and characterization of porous single-crystal-like In_2O_3 nanostructures via a solvothermal-annealing route," *Journal of the American Ceramic Society*, vol. 89, no. 2, pp. 724–727, 2006.

[18] Y. Z. Zhao, Z. X. Cheng, Q. Y. Pan, X. W. Dong, J. C. Zhang, and L. L. Pan, "Preparation and characterization of mesoporous indium oxide," *Journal of Shanghai University*, vol. 13, no. 4, pp. 292–295, 2009.

[19] C. Yu, J. Fan, B. Tian, and D. Zhao, "Morphology development of mesoporous materials: a colloidal phase separation mechanism," *Chemistry of Materials*, vol. 16, no. 5, pp. 889–898, 2004.